Journal Name

Dynamic Article Links ►

Cite this: DOI: 10.1039/c0xx00000x

www.rsc.org/xxxxxx

ARTICLE TYPE

Highly Emissive Deoxyguanosine Analogue Capable of Direct Visualization of B-Z Transition†

Soyoung Park,[a] Haruka Otomo, [a] Linjie Zheng, [a] and Hiroshi Sugiyama*[a,b,c]

Received (in XXX, XXX) Xth XXXXXXXXX 20XX, Accepted Xth XXXXXXXXX 20XX

DOI:

2-aminothieno[3,4-*d*]pyrimidine G-mimic deoxyribonucleoside, thdG, has been synthesized and incorporated readily into oligonucleotides as a versatile fluorescent guanine analogue. We demonstrate that thdG enables the visual detection of Z-DNA successfully based on different π-stacking of B- and Z-DNA.

Fluorescent probes are powerful and indispensable tools to detect biomolecules and monitor their functions. Their development is opening up new fields of research, and many biological phenomena have been understood by tracking fluorescent signals in living systems.[1] The development of fluorescent probes for nucleic acids is essential because nucleic acids are not fluorescent. In addition, a fluorescent base analogue has great significance for the expansion of an artificial genetic alphabet with diverse functionality.[2-5] Many artificial fluorescent nucleobase analogues have been developed to date and researchers are continuing to design and synthesize new forms that fulfill both isomorphicity such as native Watson–Crick base pairing and practical photophysical properties.[6-11] Recently, Tor and coworkers have developed isomorphic fluorescent RNA nucleosides derived from thieno[3,4-*d*]-pyrimidine, which have very significant photophysical features including visible light emission and a high quantum yield.[12,13] This suggested to us the potential of using such nucleobase analogues with a thienopyrimidine heterocycle and led us to exploit the thieno[3,4-*d*]-pyrimidine DNA nucleoside. Here, we focus on guanine as it plays an important role in the structural dynamics of DNA such as the formation of quadruplexes and the transition between B-DNA and Z-DNA. We describe the synthesis, photophysical properties and DNA incorporation of a fluorescent base analogue, 2-aminothieno[3,4-*d*]pyrimidine G-mimic deoxyribonucleoside, **thdG**. In addition, we have achieved successfully the direct visualization of B-Z transition using **thdG** based on different π-stacking of B- and Z-DNA.

The synthesis of **thdG** was performed by following published procedures for generating RNA nucleosides (Scheme 1).[12] The parent heterocycle with a thiophene group was synthesized from the commercially available methyl 4-aminothiophene-3-carboxylate hydrochloride (**1**) by reaction with chloroformamidine hydrochloride in dimethylsulfone at 125 °C. The amino group on 2-amino-thieno[3,4-*d*]pyrimidine-4(3*H*)-one was protected as the *N*, *N*-dimethylformamidine form. The obtained thienoguanine (**2**) could be converted into the protected deoxyribonucleoside (**3**) through Friedel–Crafts C-glycosylation with an acylated sugar derivative. This coupling afforded a mixture of β- and α-anomers with a 52% yield at β:α□proportion of 3:1. The benzoyl protecting groups were removed in a methanolic ammonia and the *N*, *N*-dimethylformamidine group was reintroduced for protection of the purine amino group. Subsequently, the 5′-hydroxyl group was protected as the dimethoxytrityl ether (DMTr) and the desired β-isomer could be isolated at a yield of 51%. The configuration at the C-1 carbons of anomers was confirmed by 1D and 2D (NOESY) ^{1}H NMR experiments (see SI).

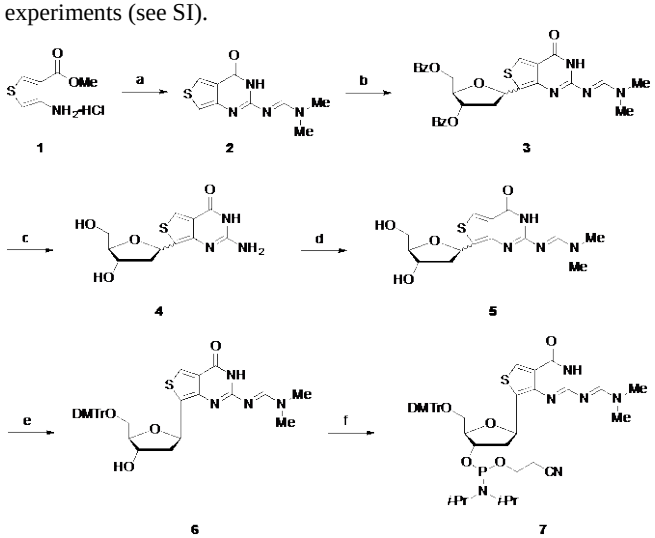

Scheme 1. Synthesis of **thdG**. Reagents and conditions: (a) (i) Chloroformamidine hydrochloride, $DMSO_2$, 125 ºC; (ii) dimethylformamide dimethyl acetal, DMF, 98%; (b) β-D-deoxyribofuranose 1-acetate 4,5-dibenzoate, $SnCl_4$, $MeNO_2$, 0 ºC to RT, 54%; (c) NH_3/MeOH, 65 ºC, 71%; (d) dimethylformamide dimethyl acetal, DMF/MeOH, 76%; (e) DMTrCl, Py, 51%; (f) 2-cyanoethyl *N*, *N*-diisopropylchloro phosphoramidite, *i*Pr_2NEt, DCM/MeCN, 0 ºC to RT.

The fundamental photophysical properties of **thdG** monomer were investigated as shown in Table 1. The fluorescence of **thdG** deoxyribonucleoside (**4**) shows absorption at 319 nm and visible emission at 455 nm with a high quantum yield under neutral conditions in water, dioxane, and MeOH. These results are similar to those of thG RNA nucleoside reported by Tor group.[12] In addition, the **thdG** deoxyribonucleoside displays a relatively higher quantum yield under dio xane (0.85) and longer excited state lifetime in water (20.5 ns) compared with a RNA nucleoside

thG. To evaluate oligonucleotides including the isomorphic dG surrogate, the phosphoramidite of **thdG** was synthesized and incorporated into the center of 18-mer DNA oligonucleotides of 5′–d(CGTCCGTC**X**TACGCACGC)–3′, where X = **thdG**, by automated solid-phase synthesis and phosphoramidite chemistry. The complementary strands of ODN1 containing matched or mismatched bases and the corresponding natural DNA duplexes with guanine were also prepared. As shown in Figure 1, the **thdG**–C base pair afforded almost identical thermal stability (T_m = 72.3 °C) compared with natural duplex DNA with a G–C base pair (T_m = 72.1 °C). A very similar tendency to decrease the Tm was observed for **thdG** (ODN1) and G (ODN2) using the complementary stands including mismatched bases (ODN3~ODN7). The thermodynamic stability and base pairing selectivity indicate that **thdG** could replace a G base in the strand without causing structural disruption. Furthermore, the fluorescent properties of ODN1 were evaluated upon hybridization with complementary strands containing matched or mismatched bases (Fig. S6). Interestingly, significant changes in the fluorescence intensity (match<T<G<A) were observed, indicating that the fluorescence of **thdG** is sensitive to local environment of DNA.[14]

Table1. Photophysical data of **thdG**

solvent	λ_{abs}/nm (ε/10^{3}M^{-1}cm^{-1})	λ_{em}/nm (ϕ)	ϕc	τ/ns	Stokes shift/cm^{-1}
water	319 (4.26)	455 (0.58)	2471	20.5	9370
dioxane	329 (5.37)	429 (0.85)	4565	14.0	7085
MeOH	327 (3.80)	460 (0.47)	1786	13.7	8842

ODN1-2:5'-CGTCCGTC**X**TACGCACGC-3' **X**=**thdG** or **G**
ODN3-7:3'-GCAGGCAG**Y**ATGCGTGCG-5' **Y**=C, T, A, G, or dSpacer

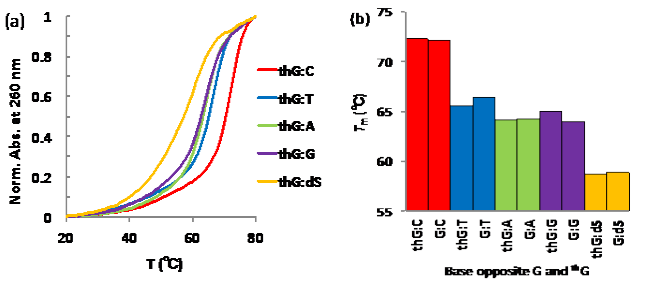

Figure 1. Thermal stability and selectivity of base pairing. (a) Thermal melts of **thG** containing DNA. ODN1:5'-CGTCCGTC**thdG**TACGCACGC -3' paired with ODN3-7:5'-GCGTGCGTA**Y**GACGGACG-3' **Y**=C, T, A, G, or dSpacer. (b) Comparison of T_m values. ODN1,2: 5' CGTCCGTC**X** TACGCACGC-3' **X**=**thdG** or **G** paired with ODN3-7. All samples contained 5 μM of each oligonucleotide strand, 20 mM Na cacodylate (pH 7.0) and 100 mM NaCl. 5'-*O*-Dimethoxytrityl-1',2'-dideoxyribose-3'-[(2-cyanoethyl)-(*N*,*N*-diisopropyl)]-phosphoramidite was used as dSpacer (dS).

The isomorphicity and the photophysical properties of **thdG** prompted us to exploit this new G-mimic deoxyribonucleoside. We intended to monitor the conformational changes of DNA through changes in fluorescence intensity of **thdG**.[15] DNA has a remarkable conformational flexibility. Among them, the most typical example is the structural transition between right-handed B-DNA and left-handed Z-DNA.[16] In particular, the dynamic structural change from the continuous π-stacks in B-DNA to the discrete four-base π-stacks in Z-DNA is a very attractive option for constructing DNA-based nanodevices.[17,18] We have demonstrated that the B–Z transition could be detected by measuring the fluorescence intensity of 2-aminopurine.[18] Based on previous studies, we expected that **thdG** fluorescence could be applied to monitor the change of electronic properties between B- and Z-DNA. To test this possibility **thdG**-containing duplex decamer, 5′–d(CGCGC**X**CGCG)–3′ (ODN8), where X = **thdG**, was prepared and investigated. However CD spectroscopy indicated that the B–Z transition became more difficult when **thdG** was incorporated as a replacement for a G nucleotide. Indeed, the duplex ODN8 produced an almost B-conformation even in 5 M NaCl. This might be explained because **thdG** favors the anti conformation and stabilizes B-form DNA when it is located in DNA oligonucleotide strands. The theoretical calculations for the syn–anti conformation of **thdG** were performed at ground state with the density functional B3LYP and the 6-31* basis set. This optimized the lowest energy conformations, suggesting that the anti conformation is more stable than the syn conformation (Figure S10). We therefore decided on the introduction of a Z-stabilizing unit into DNA sequences and 8-methylguanine (m^8G) was chosen corresponding this objective. Previously, we demonstrated that the incorporation of a methyl group at the guanine C8 position (m^8G) markedly stabilizes the Z conformation under low salt conditions. The self-complementary dodecamer d(CGC**X**C**Y**CGCG)$_2$ (ODN9), where **X** = **thdG** and **Y** = **m^8G**, was synthesized and fluorescence intensity was observed under various salt concentration. To our delight, ODN9 exhibited a dramatic change of fluorescence intensity in response to the B–Z transition. ODN9 showed typical CD spectrum of Z-DNA, a negative cotton effect around 295 nm and a positive cotton effect around 260 nm, in high salt concentrations. As shown in Figure 2, very strong fluorescence enhancement was observed in Z-DNA, whereas fluorescence was weak in B-DNA. The intense fluorescence in Z-DNA can be explained by disruption of charge transfer attributable to its four-base π-stacks (Figure S11). [18]

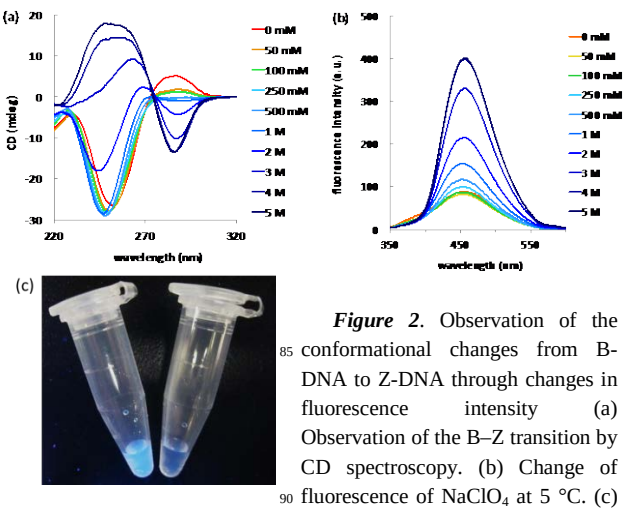

Figure 2. Observation of the conformational changes from B-DNA to Z-DNA through changes in fluorescence intensity (a) Observation of the B–Z transition by CD spectroscopy. (b) Change of fluorescence of $NaClO_4$ at 5 °C. (c) Visual detection of B–Z transition. Samples contained 5 μM of ODN9 in 20 mM sodium cacodylate buffer (pH 7.0). 5 M (left) or 50 mM (right) of $NaClO_4$ at ca. 5 °C. The photo was taken under UV irradiation.

The fluorescence of ODN9 increased proportionally when we increased the ratio of Z-conformation by adjusting the $NaClO_4$ concentration. Furthermore, as shown Figure 2c, robust brightness of ODN9 in visible region enabled to visualize B–Z transition. This inspired us with visual detection of DNA-protein interaction.[19] The DNA-binding domain of double-stranded RNA adenosine deaminase (ADAR1), called Zα domain, specifically binds to Z-DNA.[20,21] Crystal structure studies revealed that two Zα domains form a stable complex with a Z-forming CG repeat sequence.[21] Z-DNA-specific binding proteins have received attention with relevance to the influence of Z-DNA formation on transcriptional activity. We employed a Zαβ protein containing an extra Zβ domain, second Z-binding domain of ADAR1. If Zαβ is titrated into a DNA solution, the fluorescence of oligonucleotides containing **thdG** would be strongly increased in real time as B–Z transition occurs. Consequently, when we added Zαβ into the solution containing ODN9, ODN9 afforded the distinguishable bluish emission compared with the pretreated solution (Fig. 3). This indicates that oligonucleotides containing **thdG** can be a useful tool in the development of visual detection methodologies for DNA.

Figure 3. Visual detection of B-Z transition by Zαβ interaction. 4 eq. (left) or 0 eq. (right) of Zαβ was added to 1.3 μM of ODN9 and 100 mM of NaCl in 20 mM Tris-HCl buffer (pH 7.5). After incubation at 37 °C for 30 min, the photo was taken under UV irradiation.

In conclusion, **thdG** has been synthesized as a versatile fluorescent guanine analogue. It could be incorporated readily into oligonucleotides using phosphoramidite chemistry and was successfully substituted for G bases with an almost identical thermodynamic stability and base pairing selectivity. Furthermore, its remarkable photophysical properties including the strong visible emission enabled **thdG** to be applied admirably as an efficient fluorescent probe for the detection of the conformational changes in DNA. This study raises our hope that the present fluorescent nucleobase, **thdG**, could be superior to 2-Ap which is quenched in DNA and emits in the UV region.[6,22] We believe that **thdG** will expand the repertoire of fluorescent base analogues. We are currently exploring the application of **thdG** further, including its charge transfer properties and incorporation into living cells.

Notes and references

[a] *Department of Chemistry, Graduate School of Science, Kyoto University, Kitashirakawa-oiwakecho, Sakyo-ku, Kyoto 606-8502, Japan* [b]*Institute for Integrated Cell-Material Sciences (iCeMS), Kyoto University, Yoshida-ushinomiyacho, Sakyo-ku, Kyoto 606-8501, Japan* [c]*CREST, Japan Science and Technology Corporation (JST), Sanbancho, Chiyoda-ku, Tokyo 102-0075, Japan. Fax: (+)81-75-753-3670; Tel.: (+)81-75-753-4002;E-mail: hs@kuchem.kyoto-u.ac.jp*

† This communication is dedicated to Professor Andrew D. Hamilton on the occasion of his 60th birthday.

‡ Electronic Supplementary Information (ESI) available: [details of any supplementary information available should be included here]. See DOI: 10.1039/b000000x/

Acknowledgements: We express our sincere thanks for the CREST grant from the Japan Science and Technology Corporation (JST), grants from the WPI program (iCeMS, Kyoto University), and for the global COE program from the Ministry of Education, Culture, Sports, Science and Technology (MEXT), Japan.

1 a) G. Mayer, A. Heckel, *Angew. Chem., Int. Ed.* **2006**, *45*, 4900–4921; b) R. W. Sinkeldam, N. J. Greco, Y. Tor, *Chem. Rev.* **2010**, *110*, 2579–2619.
2 A. A. Henry, F. E. Romesberg, *Curr. Opin. Chem. Biol.* **2003**, *7*, 727–733.
3 S. A. Benner, *Acc. Chem. Res.* **2004** , *37*, 784–797.
4 A. T. Krueger, E. T. Kool, *Curr. Opin. Chem. Biol.* **2007**, *11*, 588–594.
5 I. Hirao, M. Kimoto, R. Yamashige, *Acc. Chem. Res.* **2012**, *45*, 2055–2065.
6 D. C. Ward, E. Reich, L. Stryer, *J. Biol. Chem.* **1969**, *244*, 1228–1237.
7 N. B. Gaied, N. Glasser, N. Ramalanjaona, H. Beltz, P. Wolff, R. Marquet, A. Burger, Y. Mély, *Nucleic Acids Res.* **2005**, *33*, 1031–1039.
8 H. Kimura, T. Katoh, T. Kajimoto, M. Node, M. Hisaki, Y. Sugimoto, T. Majima, Y. Uehara, T. Yamori, *Anticancer Res.*, **2006**, *26*, 91–97.
9 F. Seela, E. Schweinberger, K. Xu, V. R. Sirivolu, H. Rosemeyer, E.-M. Becker, *Tetrahedron* **2007**, *63*, 3471–3482.
10 Q. Xiao, R. T. Ranasinhe, A. M. P. Tang, T. Brown, *Tetrahedron* **2007**, *63*, 3483–3490.
11 M. Weinberger, F. Berndt, R. Mahrwald, N. P. Ernsting, H.-A. Wagenknecht, *J. Org. Chem.*, **2013**, *78*, 2589–2599.
12 D. Shin, R. W. Sinkeldam, Tor, Y. *J. Am. Chem. Soc.* **2011**, *133*, 14912–14915.
13 a) Y. Tor, S. D. Valle, D. Jaramillo, S. G. Srivatsan, A. Rios, H. Weizman, *Tetrahedron* **2007**, *63*, 3608–3614; b) N. J. Greco, Y. Tor, *Tetrahedron* **2007**, *63*, 3515–3527.
14 a) K.D. Kourentzi, G. E. Fox, R. C. Willson, *Anal. Biochem.*, **2003**, *322*, 124–126; b) A. A. Marti, S. Jockusch, Z. Li, J. Ju, N. J. Turro, *Nucleic Acids Res.*, **2006**, *34*, 6, e50
15 a) M. Menger, F. Eckstein, D. Porschke, *Biochemistry*, **2000**, *39*, 4500–4507; b) T. Kimura, K. Kawai, M. Fujitsuka, T. Majima, *Chem. Commun.* **2004**, *12*, 1438–1439; c) J. Li, J. J. Correia, L. Wang, J. O. Trent, J. B. Chaires, *Nucleic Acids Res.*, **2005**, *33*, 4649–4659; d) R.D. Gray, L. Petraccone, R. Buscaglia, J. B. Chaires, *Mol. Biol.*, **2010**, *608*, 121–136; e) J. Johnson, R. Okyere, A. Joseph, K. Musier-Forsyth, B. Kankia, *Nucleic Acids Res.* **2013**, *41*, 220–228.
16 a) A. Rich, A. Nordheim, A. H.-J. Wang, *Ann. Rev. Biochem.* **1984**, *53*, 791–846; b) T. M. Jovin, D. M. Soumpasis, L. P. McIntosh, *Ann. Rev. Phys. Chem.* **1987**, *38*, 521–560.
17 a) C. Mao, W. Sun, Z. Shen, N. C. Seeman, *Nature*, **1991**, *397*, 144–146; b) L. Feng, A. Zhao, J. Ren, X. Qu, *Nucleic Acids Res.*, **2013**, *41*, 7987–7996.
18 a) R. Tashiro, H. Sugiyama, *Angew. Chem. Int. Ed.* **2003**, *42*, 6018–6020; b) R. Tashiro, H. Sugiyama, *J. Am. Chem. Soc.* **2005**, *127*, 2094–2097.
19 a) T. D. Bradrick, J. P. Marino, *RNA*, **2004**, *10*, 1459–1468; b) G. Tamulaitis, M. Zaremba, R. H. Szczepanowski, M. Bochtler, V. Siksnys, *Nucleic Acids Res.*, **2007**, *35*, 4792–4799; c) L. J. Reha-Krantz, *Mol. Biol.*, **2009**, *521*, 381–396; d) L. J. Reha-Krantz, C. Hariharan, U. Subuddhi, S. Xia, C. Zhao, J. Beckman, T. Christian, W. Konigsberg, *Biochemistry*, **2011**, *50*, 10136–10149.
20 T. Schwaltz, M. A. Rould, K. Lowenhaupt, A. Herbert, A. Rich, *Science*, **1999** , *284*,1841–1845.
21 S. Bae, D. Kim, K. K. Kim, Y. Kim, S. Hohng, *J. Am. Chem. Soc.*, **2011**, *133*, 668–671.
22 a) J. M. Jean, K. B. Hall, *Proc. Natl. Acad. Sci. USA* **2001**, *98*, 37–41; c) N. P. Johnson, W. A. Baase, P. H. Hippel, *Proc. Natl. Acad. Sci. USA* **2004**, *101*, 3426–3431.

Supporting Information

Highly Emissive Deoxyguanosine Analogue Capable of Direct Visualization of B-Z Transition†

Soyoung Park,[†] Haruka Otomo,[†] Linjie Zheng,[†] and Hiroshi Sugiyama*[,†,‡,§]*

[†]Department of Chemistry, Graduate School of Science, Kyoto University, Kitashirakawa-oiwakecho, Sakyo-ku, Kyoto 606-8502, Japan

[‡]Institute for Integrated Cell-Material Sciences (iCeMS), Kyoto University, Yoshida-ushinomiyacho, Sakyo-ku, Kyoto 606-8501, Japan

[§]CREST, Japan Science and Technology Corporation (JST), Sanbancho, Chiyoda-ku, Tokyo 102-0075, Japan

**Corresponding author:* Dr. Soyoung Park, Prof. Dr. Hiroshi Sugiyama

Tel.: (+)81-75-753-4002; Fax: (+)81-75-753-3670

E-mail: oleesy@kuchem.kyoto-u.ac.jp, hs@kuchem.kyoto-u.ac.jp (H.S.)

Materials used for synthesis of thdG

$DMSO_2$, $MeNO_2$, *N*, *N*-dimethylformamide dimethyl acetal, 2-cyanoethyl *N*,*N*-diisopropylchloro phosphoramidite and dimethoxytrityl chloride were received from Wako Chemicals and used without further purification. $SnCl_4$ was purchased from Sigma-Aldrich Chemicals Co. (Milwaukee, WI). 2.0 M ammonia in methanol was received from TCI. Methyl 4-aminothiophene-3-carboxylate hydrochloride was purchased from Apollo Scientific Ltd. All other chemicals and solvents were purchased from Sigma-Aldrich Chemicals Co., Wako Pure Chemical Ind. Ltd., TCI, or Kanto Chemical Co. Inc. ß-D-deoxyribofuranose 1-acetate 4,5-dibenzoate and Chloroformamidine hydrochloride were prepared by following the literature procedures [1, 2]. Water was deionized (specific resistance of ≥ 18.0 MΩ cm at 25 °C) by a Milli-Q system (Millipore Corp.).

Methods used for synthesis of thdG

NMR spectra were obtained on a JEOL JNM ECA-600 spectrometer operating at 600 MHz for ^{1}H NMR and in $CDCl_3$ unless otherwise noted. Flash column chromatography was performed employing Silica Gel 60 (70–230 mesh, Merck Chemicals). Silica-gel preparative thin-layer chromatography (PTLC) was performed using plates from Silica gel 70 PF_{254} (Wako Pure Chemical Ind. Ltd.).

Synthesis of thdG and its phosphoramidite

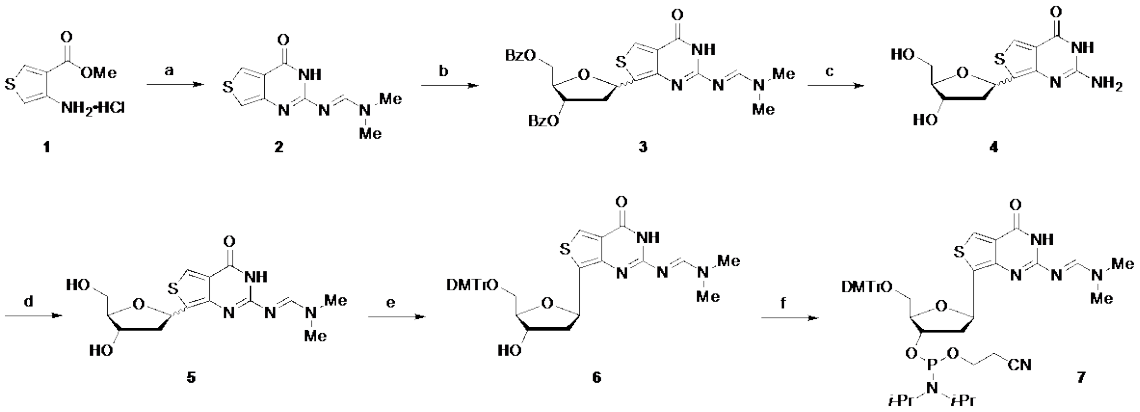

Reagents and conditions: (a) (i) Chloroformamidine hydrochloride, $DMSO_2$, 125 ºC; (ii) dimethylformamide dimethyl acetal, DMF, 98%; (b) β-D-deoxyribofuranose 1-acetate 4,5-dibenzoate, $SnCl_4$, $MeNO_2$, 0 ºC to RT, 54%; (c) NH_3/MeOH, 65 ºC, 71%; (d) dimethylformamide dimethyl acetal, DMF/MeOH, 76%; (e) DMTrCl, Py, 51%; (f) 2-cyanoethyl *N*, *N*-diisopropylchloro phosphoramidite, *i*Pr_2NEt, DCM/MeCN, 0 ºC to RT

***N*^{2}-DMF 2-aminothieno[3,4-*d*]pyrimidine G mimic 3,5-di-*O*-benzoyldeoxynucleoside (3)**

N^2-DMF 2-aminothieno[3,4-*d*]pyrimidin-4(3*H*)-one(**2**) was prepared from methyl 4-aminothiophene-3-carboxylate hydrochloride(**1**) as reported previously.[1] To a suspension of *N*^{2}-DMF 2-aminothieno[3,4-*d*]pyrimidin-4(3*H*)-one (1.1 g, 4.7 mmol) and β-D-deoxyribofuranose 1-acetate 4,5-dibenzoate[2] (1.9 g, 5.0 mmol) in dry $MeNO_2$ (20 mL) was dropwise added $SnCl_4$(1.2 mL, 10 mmol) over 10 min at 0 ºC and stirred for 10 min at the same temperature. Removed from ice bath and after 3 h stirring at room temperature, β-D-deoxyribofuranose 1-acetate 4,5-dibenzoate(0.97 g, 2.5 mmol) was added to the reaction mixture and then was stirred overnight. Sat. aq. $NaHCO_3$ was added to the mixture and diluted with CH_2Cl_2. The resulting mixture was vigorously stirred for 1.5 h and the preticipate was filtered over a Celite cake. The separated aq. layer was extracted with CH_2Cl_2. The combined layer were dried over $MgSO_4$ and evaporated. The residue was purified by column chromatography with CH_2Cl_2:MeOH = 35:1 to afford a brown product (1.4 g, 54%, mixture of β/α = 3/1). ^{1}H NMR of β-anomer (600 MHz, $CDCl_3$): δ 8.66 (s, 1H), 8.40 (s, 1H), 8.12-8.06 (m, 5H), 7.62-7.55 (m, 2H), 7.49-7.36 (m, 4H), 5.97-5.94 (m, 1H), 5.71 (m, 1H), 4.65-4.54 (m, 4H), 3.16 (s, 3H),

3.07 (s, 3H); ESI-HRMS calculated for $C_{28}H_{27}N_4O_6S$ $[M^+H]^+$ 547.1651, found 547.1691.

2-Aminothieno[3,4-*d*]pyrimidine G mimic deoxynucleoside (4)

A solution of **3** (1.6 g, 2.9 mmol) in 2.0 M ammonia (150 mL) in methanol was heated at 65 ºC overnight. In brown reaction mixture, white solid appeared and then dissolved. The mixture was evaporated and purified by column chromatography with CH_2Cl_2:MeOH = 35:1 to afford a brown oil. (540 mg, 65%, mixture of β/α = 3/1) ^{1}H NMR of β-anomer (600 MHz, DMSO-d_6): δ 10.49 (s, 1H), 8.12 (s, 1H), 6.12 (s, 2H), 5.56 (dd, J = 10.54, 5.14 Hz, 1H), 5.05 (d, J = 3.45 Hz), 4.80 (s, 1H), 4.20 (s, 1H) ,3.74-3.72 (m, 1H), 3.44-3.33 (m, 2H), 1.92-1.87 (m, 1H); ESI-HRMS calculated for $C_{11}H_{14}N_3O_4S$ $[M^+H]^+$ 284.0705, found 284.0598.

***N*^{2}-DMF-2-aminothieno[3,4-*d*]pyrimidine G mimic deoxynucleoside (5)**

A solution of **4** (540 mg, 1.9 mmol) and *N, N*-dimethylformamide dimethyl acetal (0.38 mL) in DMF/MeOH (1/1, 24 mL) was stirred overnight at RT. All volatiles were evaporated, and the oily residue was coevaporated with DMF (2 × 2 mL). The residue was purified by column chromatography with CH_2Cl_2:MeOH = 35:1 to afford a yellow solid (26 mg, 87 %, mixture of β/α = 3/1). ^{1}H NMR of β-anomer (600 MHz, DMSO-d_6): δ 10.99 (s, 1H), 8.54 (s, 1H), 8.16 (s, 1H), 5.66 (dd, J = 10.19, 5.46 Hz, 1H),5.11 (d, J = 4.10 Hz, 1H), 4.80 (t, J = 5.46 Hz, 1H), 4.23 (m, 1H), 3.77-3.75 (m, 1H), 3.48-3.38 (m, 2H), 3.15 (s, 3H), 3.02 (s, 3H), 2.18-2.15 (m, 1H), 2.02-1.97 (m, 1H); ESI-HRMS calculated for $C_{14}H_{19}N_4O_4S$ $[M^+H]^+$ 339.1127, found 339.1153.

***O*$^{5'}$-Dimethoxytrityl-*N*^{2}-DMF-2-aminothieno[3,4-*d*]pyrimidine G mimic deoxynucleoside (6)**

5 (50 mg, 0.15 mmol) was coevaporated with dry pyridine (2 × 1 mL). DMTrCl (60 mg, 0.18 mmol) in dry pyridine (0.3 mL) was added and the solution was stirred at RT for 3 hours. The reaction mixture was directly loaded on silica pad for column chromatography with CH_2Cl_2:MeOH = 1:0 to 10:1 containing 1.5 % triethylamine to afford an off-white solid (48 mg, 51 %). ^{1}H NMR of β-anomer (600 MHz, $CDCl_3$): δ 8.67 (s, 1H), 8.19 (s, 1H), 8.09 (s, 1H), 7.47 (d, J = 8.31 Hz, 2H), 7.35 (dd, J = 8.85, 3.39 Hz, 4H), 7.28-7.26 (m, 2H), 7.21-1.18 (m, 1H), 6.81 (d, J = 8.20, 4H), 5.95 (dd, J

= 10.20, 5.44 Hz, 1H), 4.50 (m, 1H), 4.05 (m, 1H), 3.78 (s, 6H), 3.29 (m, 2H), 3.15 (d, *J* = 2.73 Hz, 3H), 3.05 (d, *J* = 2.67 Hz, 3H), 2.40 (ddd, *J* = 13.43, 5.61, 2.04 Hz, 1H), 2.28 (ddd, *J* = 13.26, 10.20, 6.12 Hz, 1H), 1.93 (s, 1H); ESI-HRMS calculated for $C_{35}H_{37}N_4O_6S$ $[M^+H]^+$ 641.2434, found 641.2494.

(3'-(2-Cyanoethyldiisopropylphosphoramidite)-*O*$^{5'}$-dimethoxytrityl-*N*^{2}-DMF-2-aminothieno [3,4-*d*]pyrimidine G mimic nucleoside (7)

6 (50 mg, 0.080 mmol) was coevaporated with dry pyridine (2 × 1 mL), dried under vacuum for 3 h, and dissolved in 0.7 mL of dry CH_2Cl_2. *N, N*-diisopropylethylamine (0.041 mL, 0.24 mmol) and 2-cyanoethyl *N*,*N*-diisopropylchlorophosphoramidite (0.035 mL, 0.16 mmol) were successively added to the solution at 0 ^oC, and the reaction mixture was allowed to warm up and stirred 3 h at RT. All volatiles were then evaporated and without further purification the residue dissolved in CH_2Cl_2/MeCN (1/3, 0.5 mL) for DNA solid synthesis.

Figure S1. NMR spectra of **6** (β- and α-anomer). (a) ^{1}H NMR spectrum of **6** (β-anomer) (b) COSY spectrum of **6** (β-anomer) (c) NOESY spectrum of **6** (β-anomer) (d) ^{1}H NMR spectrum of **6** (α-anomer) (e) COSY spectrum of **6** (α-anomer) (f) NOESY spectrum of **6** (α-anomer)

(a) 1H NMR spectrum of **6** (β-anomer)

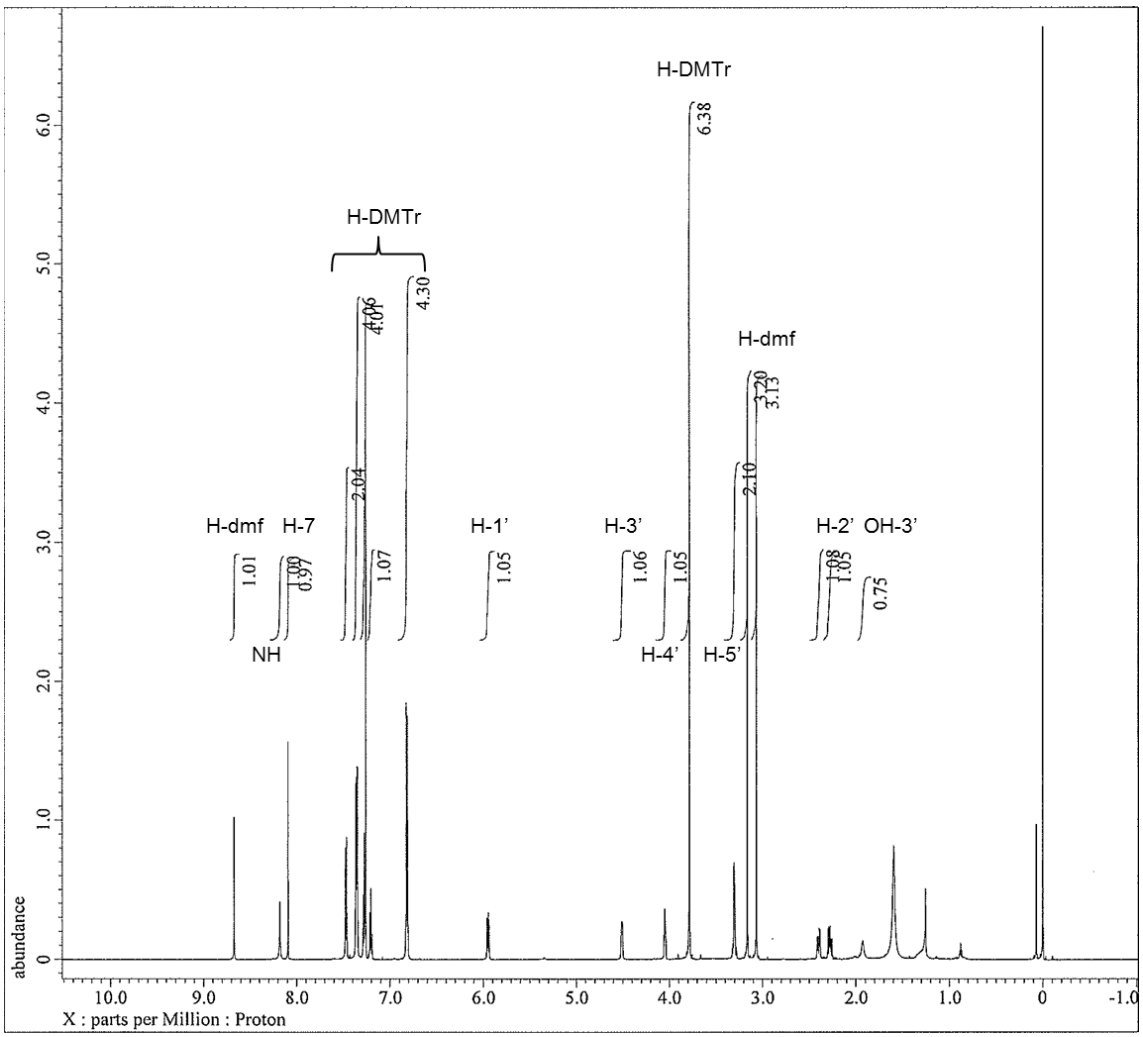

(b) COSY spectrum of **6** (β-anomer)

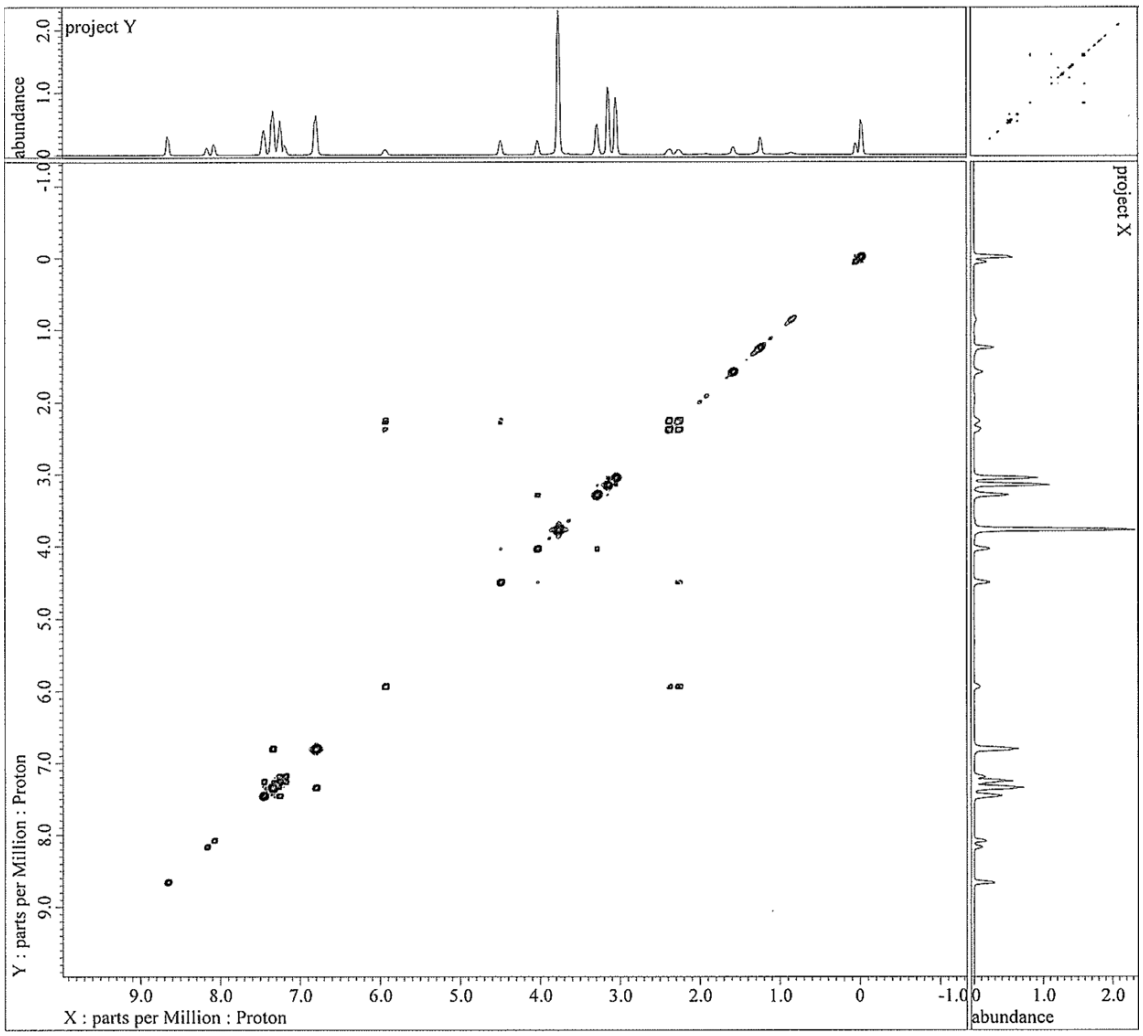

(c) NOESY spectrum of **6** (β-anomer)

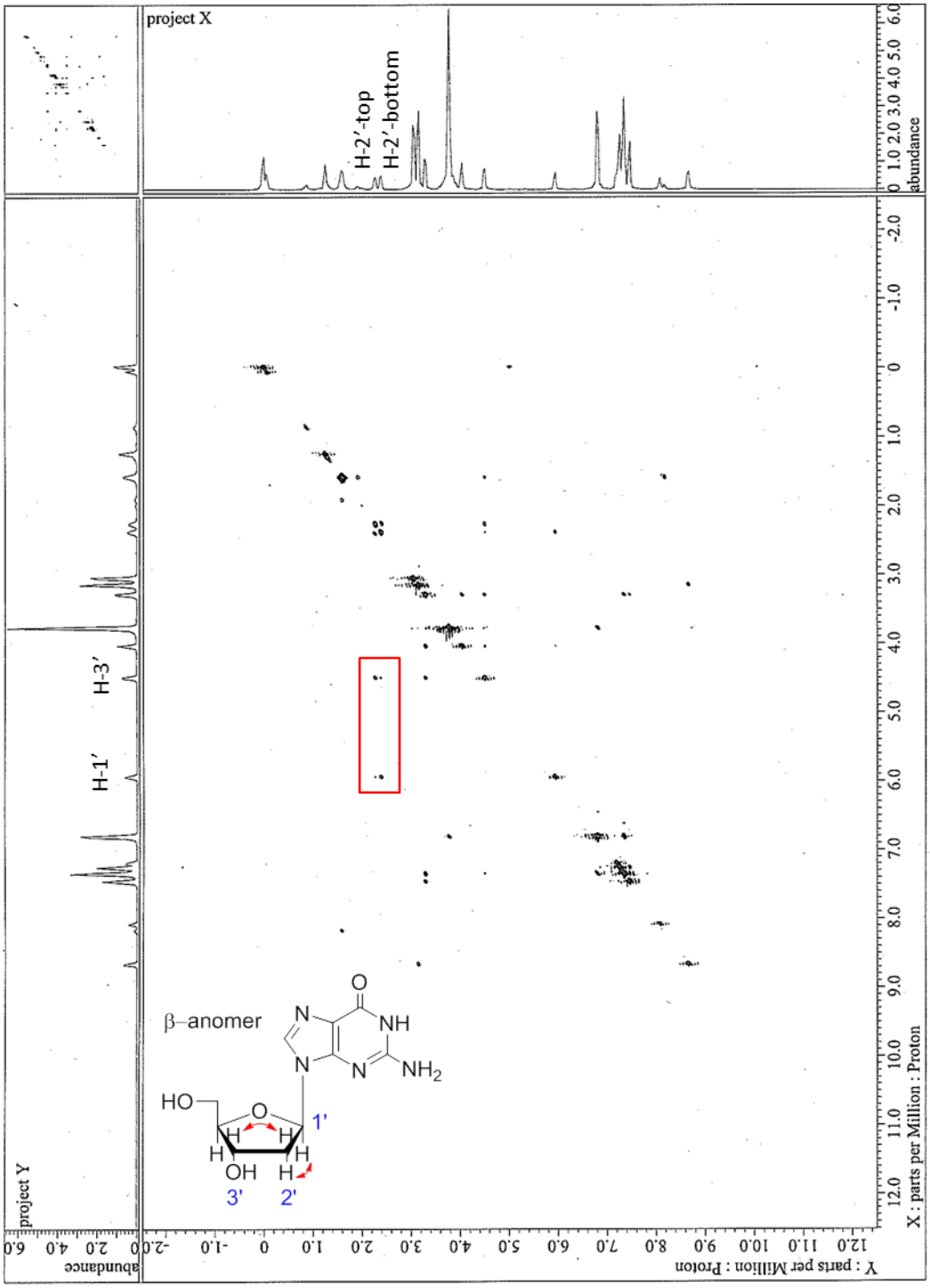

(d) 1H NMR spectrum of **6** (α-anomer)

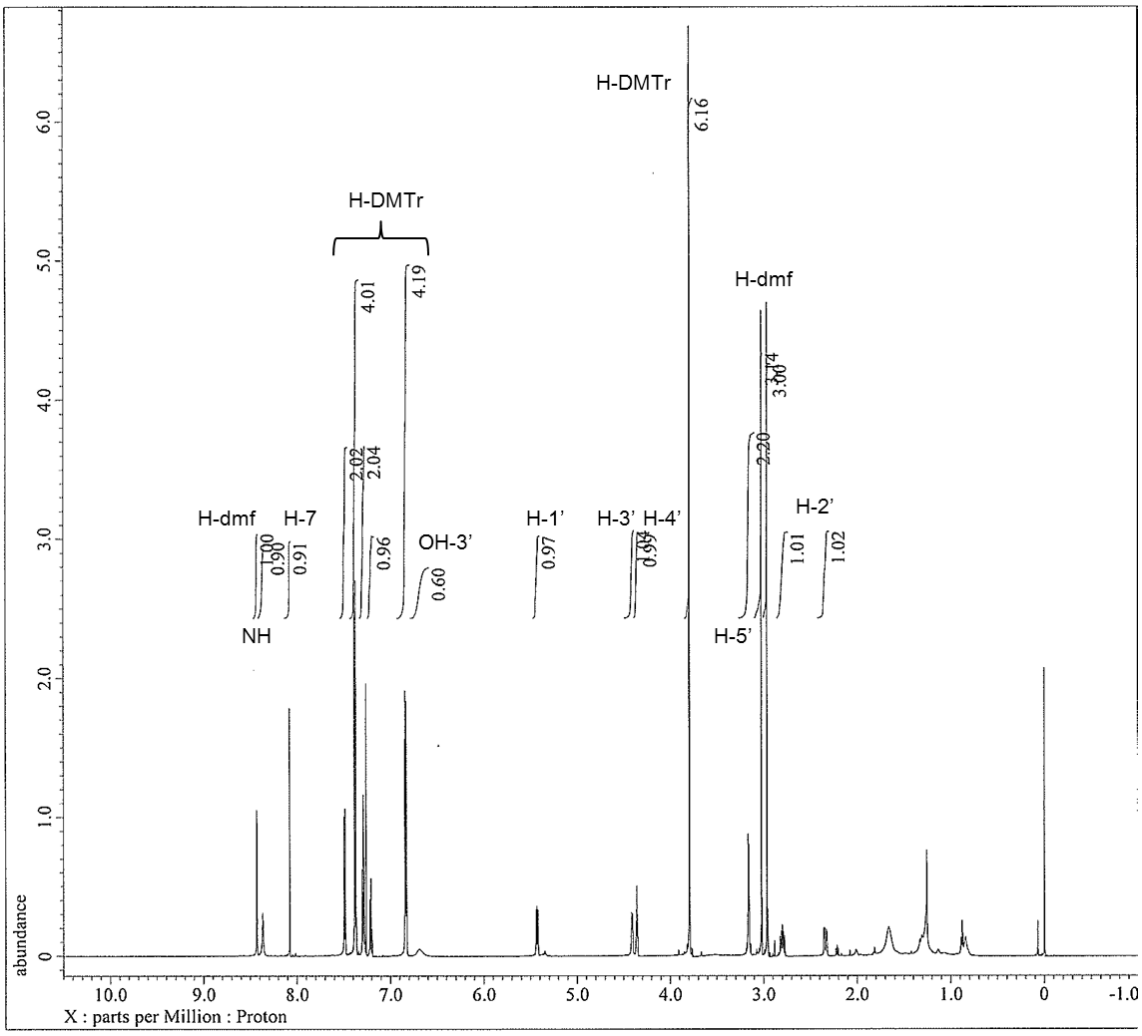

(e) COSY spectrum of **6** (α-anomer)

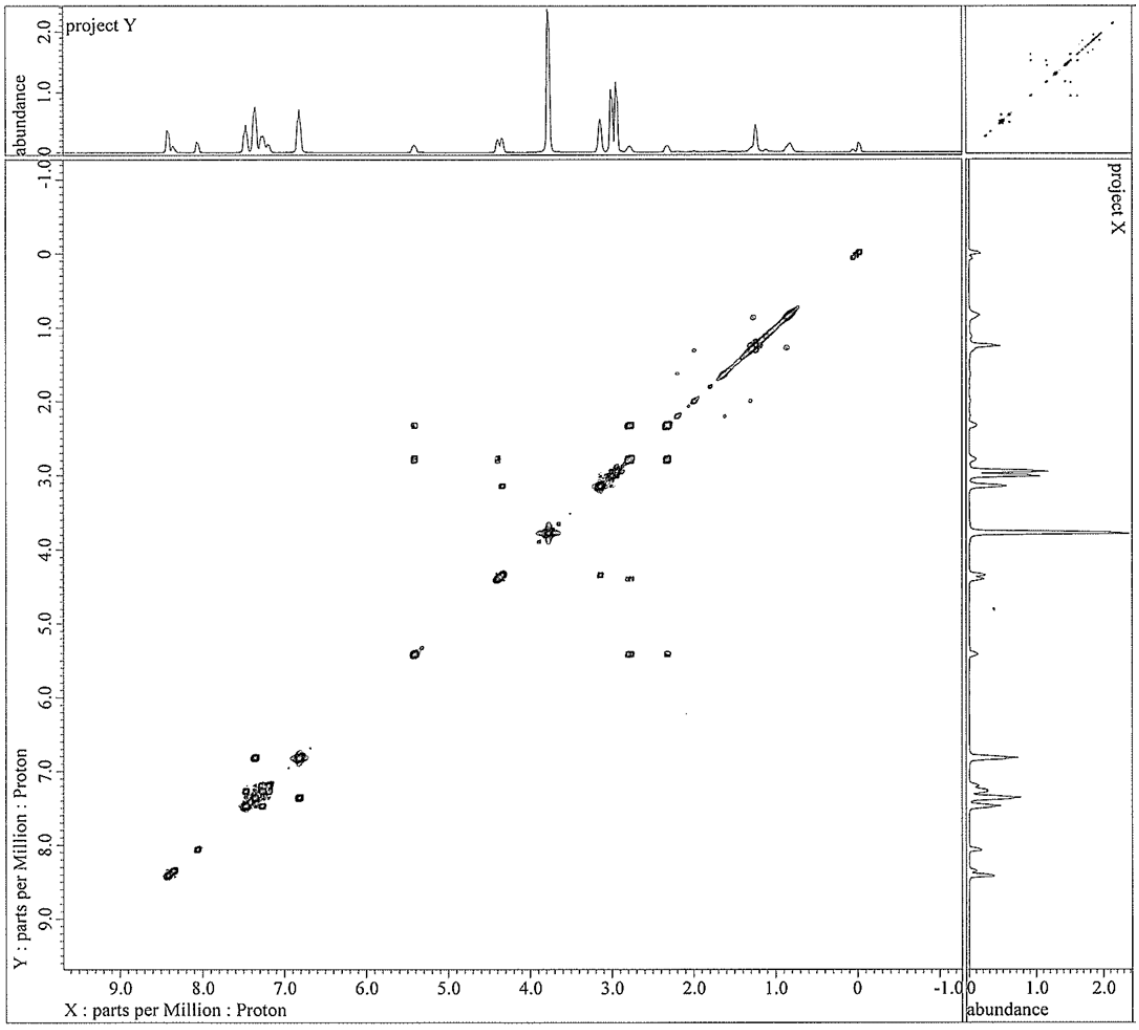

(f) NOESY spectrum of **6** (α-anomer)

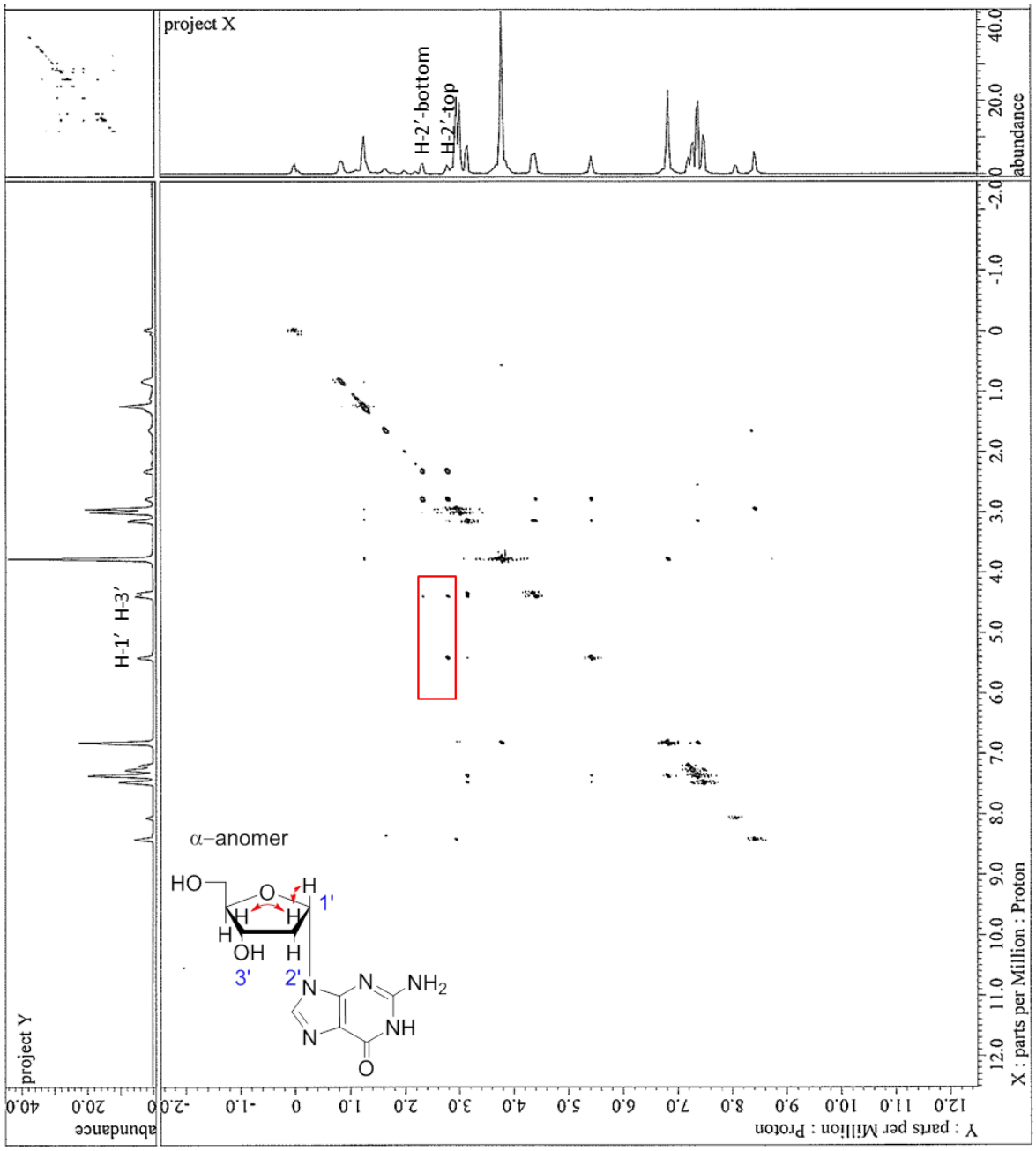

Photophysical data for thdG monomer

Samples were studied in water, dioxane, and MeOH at 20 °C. All samples were prepared from a DMSO stock solution. Measurement was conducted with 10 μM thG monomer in the each solvent containing trace DMSO. All experiments were performed in duplicate with negligible differences; hence only one series is shown.

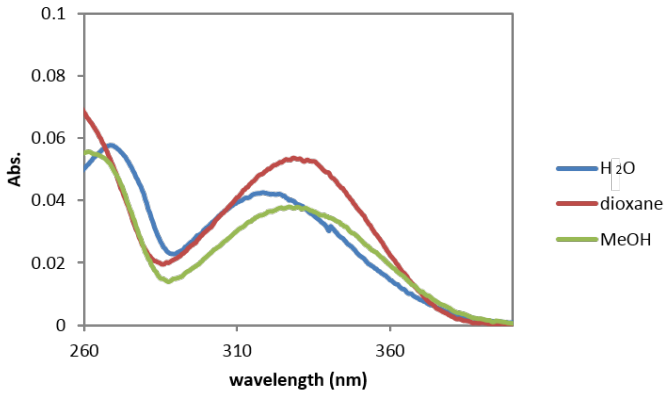

Figure S2. JASCO V-650 UV/VIS spectrophotometer was used to record absorption spectra with a 0.5 nm resolution. The cuvette temperature was kept at 25 °C by JASCO PAC-743R. Samples were prepared with 10 μM in H_2O, dioxane, or MeOH (blue, red, or green line).

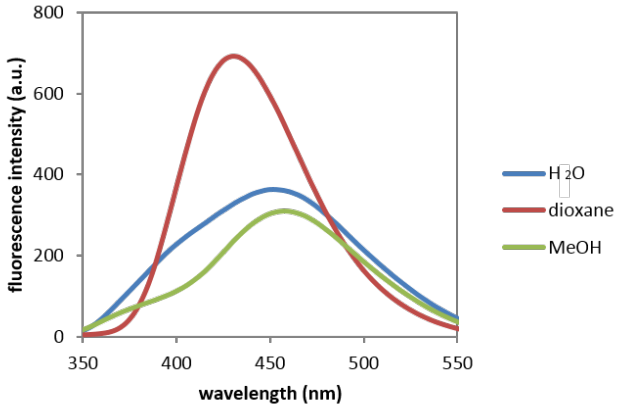

Figure S3. Fluorescence measurements were conducted using a JASCO FP-6300 spectrofluorometer. The sample temperature was controlled with a JASCO EHC-573 at 25 °C. Measurements were performed using fluorescence cells with a 0.5-cm path length. The result of the sample dissolved in H_2O is shown as a blue line, dioxane is red line, and MeOH is green line.

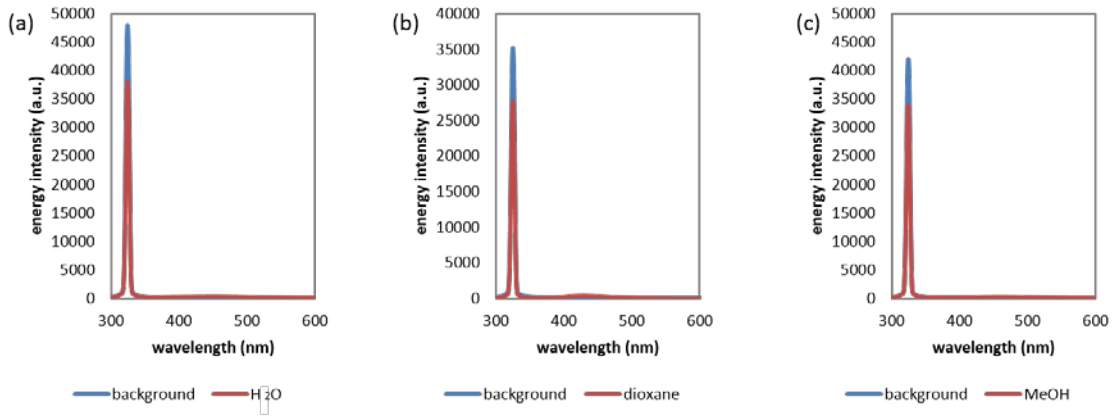

Figure S4. Quantum yields were measured with HAMAMATSU Absolute PL Quantum Yield spectrometer C11347. Samples were dissolved in (a) H_2O (b) dioxane (c) MeOH. All samples were excited at 325 nm. In addition, ODN9 in 20 mM sodium cacodylate buffer (pH 7.0) and 0 M or 5 M of $NaClO_4$ at 25 °C exhibit very low quantum yields of 0.023 and 0.062. This suggests that ODN9 convert some of the absorption at 260 nm into the emission.

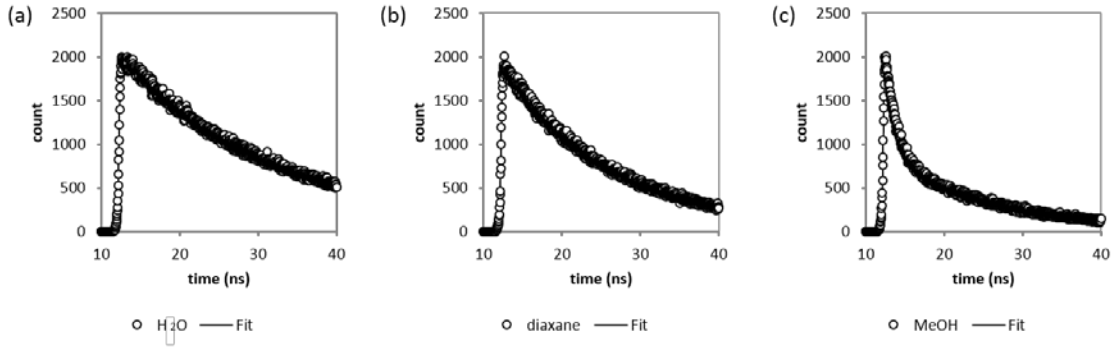

Figure S5. Fluorescence decay curves were collected on a HORIBA Fluorocube 3000U-SHK using an LED laser source for excitation. All samples were excited at 325 nm and the fluorescence decay was observed at 450 nm. Decay curves were fitted using three exponential functions. Samples were dissolved in (a) H_2O (b) dioxane (c) MeOH.

Solid-Phase Synthesis

ODNs having thdG (ODN1, 8, 9) were synthesized on solid supports using (3'-(2-Cyanoethyldiisopropylphosphoramidite)-$O^{5'}$-dimethoxytrityl-N^2-DMF-2-aminothieno [3,4-d]pyrimidine G mimic nucleoside (7) and commercially available $O^{5'}$- dimethoxytrityl -2'-deoxyribonucleoside $O^{3'}$-phosphoramidites. Solid-phase oligonucleotide synthesis was performed on an ABI DNA synthesizer (Applied Biosystem, Foster City, CA). The modified phosphoramidite was chemically synthesized as described above and without purification incorporated into oligonucleotide through coupling reaction for 10 minutes. Cleavage from the solid support and deprotection were accomplished with 50:50 of $MeNH_2$ in 40 wt. % in water and NH_3 in 28 wt. % in water at rt for 15 min and then at 65 °C for 15 min. After purification by HPLC, products were confirmed by ESI-TOFMS (Table S1). DNA concentrations were determined by using the Nano drop ND-1000 (Nano-drop Technologies, Wilmington, DE).

Table S1. ESI-TOF-Mass data of ODNs.

	calcd.	found
ODN1 $[M-4H]^{-4}$	1361.7	1362.3
ODN8 $[M-3H]^{-3}$	1013.8	1014.0
ODN9 $[M-3H]^{-3}$	1018.5	1018.7

Other ODNs are received from SIGMA-Genosys or JBios.

UV-melting

Melting temperatures were determined by measuring changes in absorbance at 260 nm as a function of temperature using a JASCO V-650 UV/VIS spectrophotometer. JASCO PAC-743R equipped with a high performance temperature controller and micro auto eight-cell holder. Absorbance was recorded in the forward and reverse direction at temperatures from 5 to 95 °C at a rate of 0.5 °C/min. The melting samples were denatured at 95 °C for 5 min and annealed slowly to RT then stored at 5 °C until experiments were initiated. All melting samples were prepared in a total volume of 100 μL containing 5 μM of each strand oligonucleotide, 20 mM Na cacodylate (pH 7.0) and 100 mM NaCl. Synthetic oligonucleotides were obtained from Sigma-Aldrich Chemicals Co.

Fluorescence Measurement

Fluorescence measurements of th**dG**-containing DNA were conducted using a JASCO FP-6300 spectrofluorometer. The sample temperature was controlled with a JASCO EHC-573. Measurements were performed using fluorescence cells with a 0.5-cm path length. All samples are containing 5 μM of each strand oligonucleotide in 20 mM sodium cacodylate buffer (pH 7.0) and various concentrations of $NaClO_4$ at 5 °C.

CD Spectroscopy

CD spectra of oligonucleotide solutions collected in 0.5-nm steps from 320 to 220 nm were measured using JASCO J-805LST Spectrometer in a 1-cm quartz cuvette. The buffer and concentrations of $NaClO_4$ were the same as for Fluorescence measurement. Each spectrum shown is the average of two individual scans.

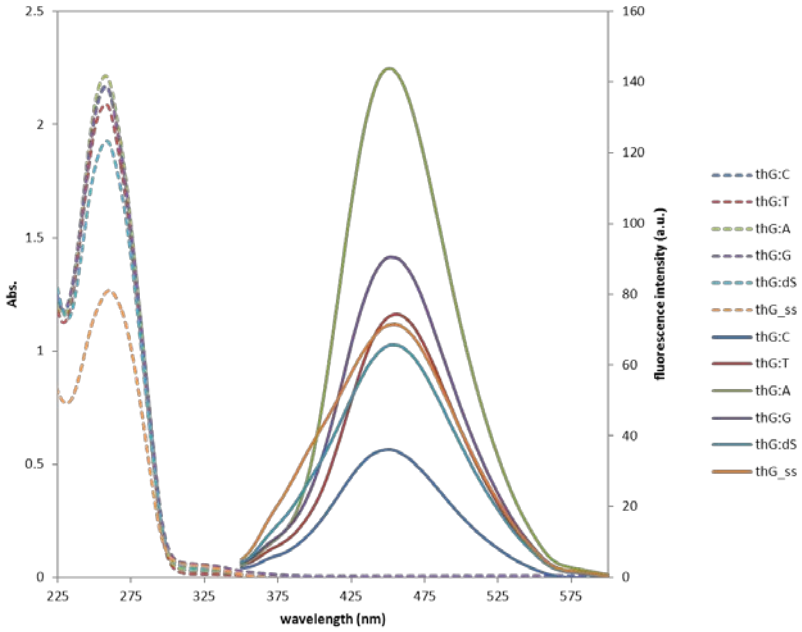

Figure S6. Fluorescent properties of ODN1 hybridized with complementary strands containing matched or mismatched bases.

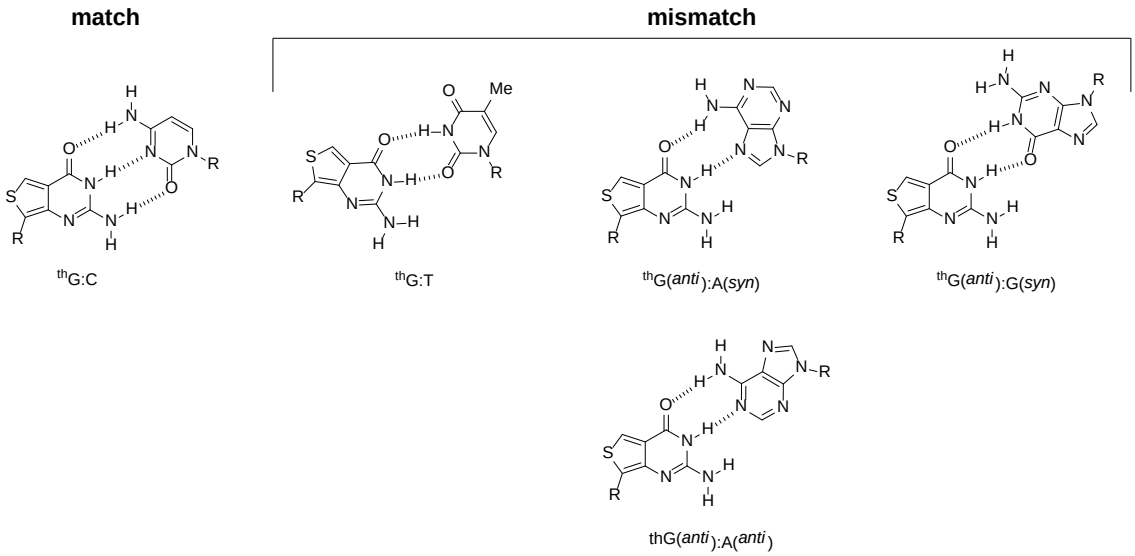

Figure S7. Plausible hydrogen-bonding of **thdG** and match or mismatch bases [3, 4].

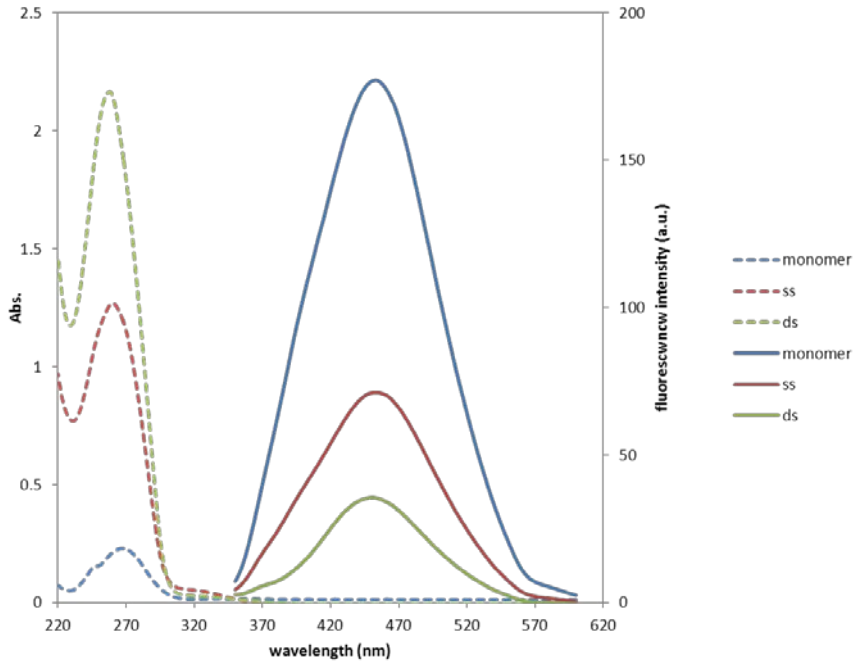

Figure S8. Fluorescent properties of th**dG** monomer and ODN1.

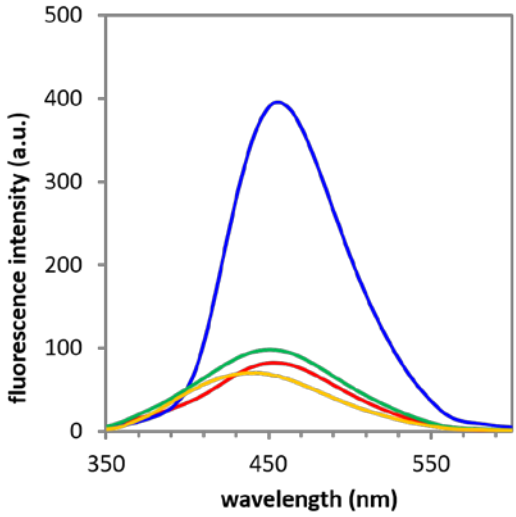

	solute	$NaClO_4$	T
dsDNA (B)	ODN9	50 mM	5 ℃
dsDNA (Z)	ODN9	5 M	5 ℃
ssDNA	ODN9	5 M	70 ℃
Monomer	monomer	0 mM	5 ℃

Figure S9. Fluorescent properties of th**dG** monomer and ODN9 (single strand, B- or Z-form) Samples are containing 10 μM of DNA or monomer in sodium cacodylate buffer (20 mM, pH = 7.0)

Density Functional theory (DFT) and *Ab initio* Calculations

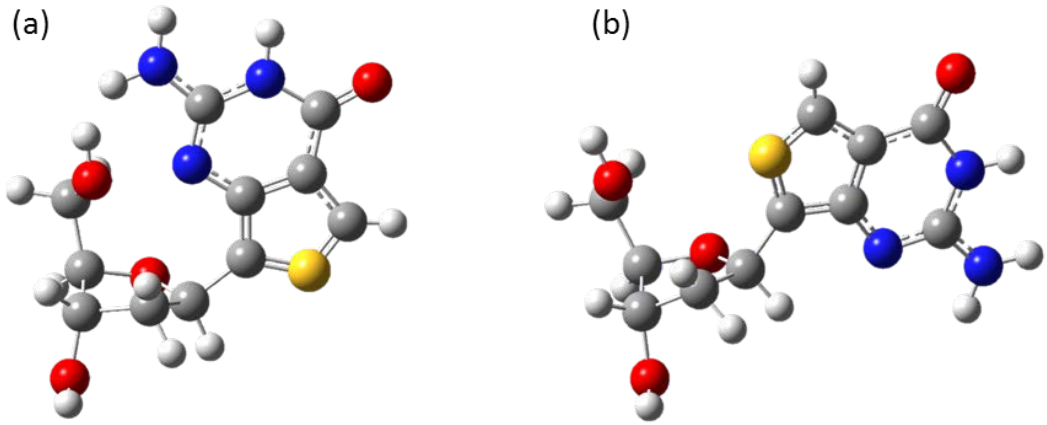

Figure S10. Optimized formation of (a) syn-th**dG** and (b) anti-th**dG**. The structures reported here were optimized using B3LYP method and 6-31G* basis set. Since B3LYP method and 6-31G* basis set have been shown to be effective for the investigation of biomolecules. All the calculations reported here were carried out at gas phase using the Gaussian 09W software. Energies of syn-th**dG** is -805773.46 kcal/mol. anti-th**dG** is -805723.12 kcal/mol. Anti-th**dG** is more stable than syn-th**dG** by 45.34 kcal/mol.

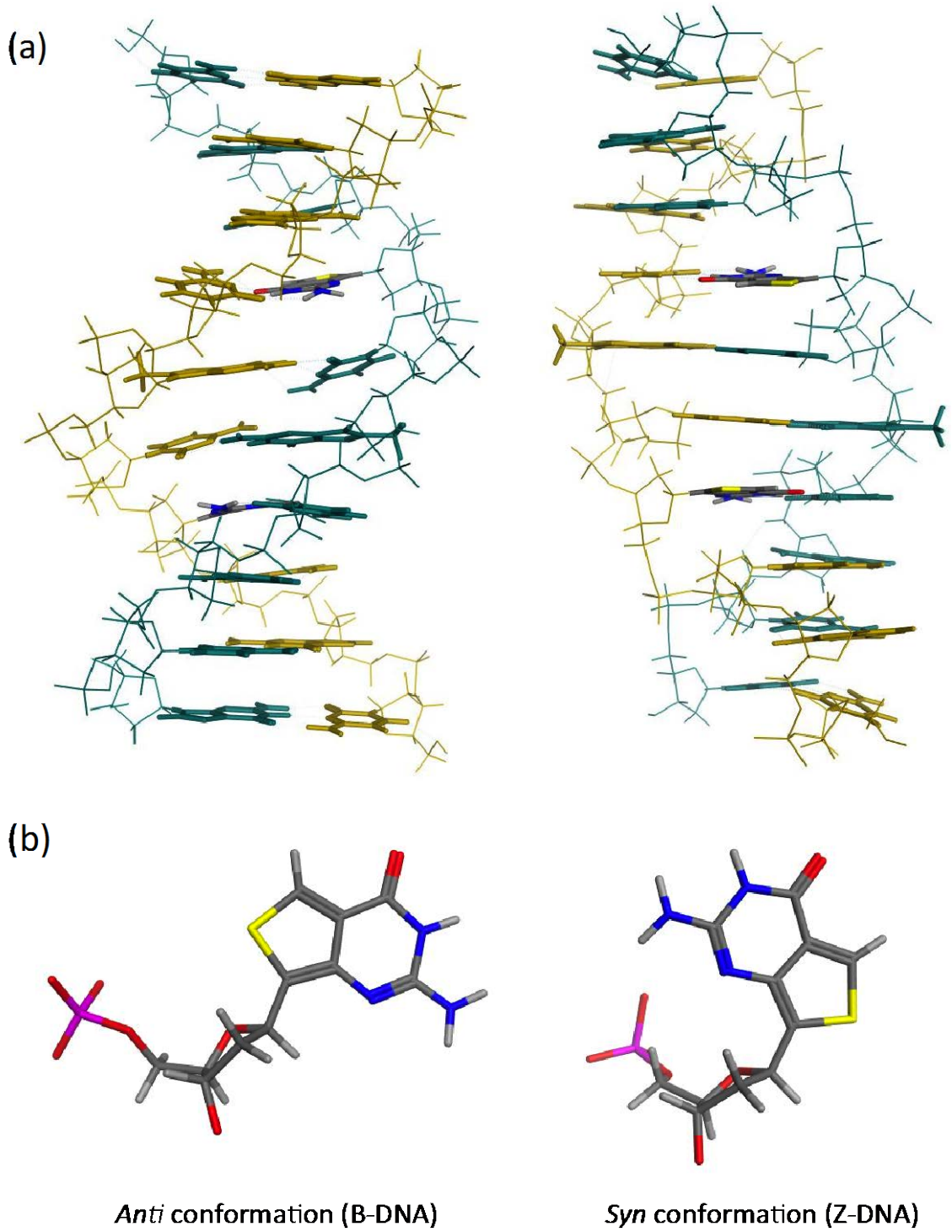

Figure S11. (a) Molecular models of B-form (left) and Z-form DNA of ODN9 (right). The sulfur atoms of **thdG** are drawn in yellow. (b) *Syn* and *anti* conformation of thieno[3,4-*d*]-pyrimidine relative to the sugar in nucleotides. The Energy minimizations were performed using the MOE (Molecular Operating Environment). DNA structures were made using AMBER forcefield and the dielectric constant $\varepsilon=4r_{ij}$.

Preparation of Zαβ protein.

Zαβ domain of ADAR1 was expressed using a plasmid (pET21a-Zαβ) containing a subcloned Zαβ domain. pET21a-Zαβ was transformed to an *E. coli* BL21 (DE3) competent cell. Small cultured cell was grown in a 500 ml of LB medium with ampicillin (100 μg/ml) at 37 ^{o}C for 2 h, and then the target protein was induced with 0.5 mM IPTG at 30 ^{o}C for 6 h. The cell was harvested by centrifuge at 9,000 rpm for 5 min, then the collected pellet was resuspended in a 50 mM Tris-HCl buffer (pH 8.0) containing 300 mM NaCl. After sonication and centrifuge at 15,000 rpm for 30 min at 4 ^{o}C, the supernatant was incubated with Ni-NTA beads for 2 h. The beads were washed, and then the bound protein was eluted with increasing concentrations of imidazole (50, 100, 200, and 400 mM; 1.0-ml fractions). The eluted protein sample (usually 200 mM fraction) was dialyzed against 20 mM Tris-HCl (pH 7.5) and 20 mM NaCl. The concentration was determined by BCA method.

Visual detection of B-Z transition by Zαβ interaction

0-20 equivalent of Zαβ was added to 1.3 μM of ODN9 and 100 mM of NaCl in 20 mM Tris-HCl buffer (pH 7.5). After incubation at 37 °C for 30 min, the photo was taken under UV irradiation. For the visualization of the dynamic change of the color, relatively high concentration of DNA solution was used. CD spectroscopy and fluorescence measurement were also observed (Figure S12). To investigate the possibility that Zαβ increased the fluorescence without B-Z transition, 0 or 4 equivalent of Zαβ was added to 1.3 μM of ODN1 (B-form) and 100 mM of NaCl in 20 mM Tris-HCl buffer (pH 7.5). After incubation at 37 °C for 30 min, fluorescence measurement was conducted (Figure S13). Consequently, we found that Zαβ did not induce the big difference on the fluorescence compared with B-Z transition.

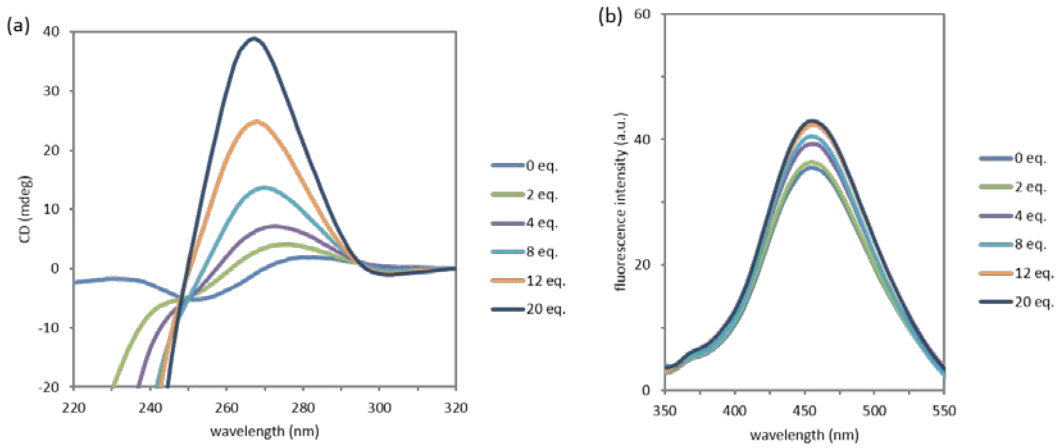

Figure S12. CD spectra and fluorescence properties of ODN9 with 0-20 equivalent of Zαβ.

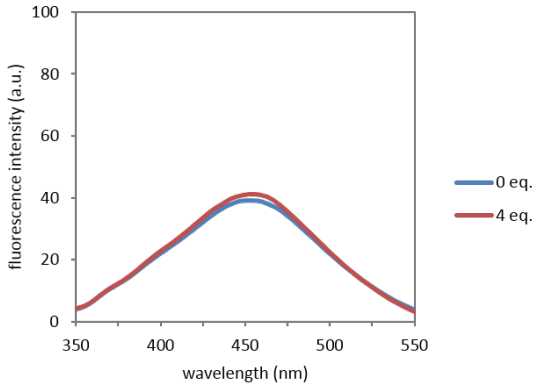

Figure S13. Fluorescence properties of ODN1 with 0 or 4 equivalent of Zαβ.

References :

[1] D. Shin, R. W. Sinkeldam, Y. Tor, *J. Am. Chem. Soc.*, 2011, **133**, 14912.

[2] C. Génu-Dellac, G. Gosselin, J.-L. Imbach, *Carbohydr. Res.*, 1991, **216**, 249.

[3] T. Brown, *Aldrichimica Acta*, 1995, **28**, 15

[4] A. Lane, B. Peck, *Eur. J. Biochem.*, 1995, **230**, 1073